EXAFS and X-ray Powder Diffraction Studies of the Spin Transition Molecular Materials $[Fe(Htrz)_2(trz)](BF_4)$ and $[Fe(Htrz)_3](BF_4)_2 \cdot H_2O$ (Htrz = 1,2,4-4*H*-triazole; trz = 1,2,4-triazolato)

Alain Michalowicz,*[,†,‡] Jacques Moscovici,[‡] Bernard Ducourant,[§] Denis Cracco,[⊥] and Olivier Kahn*[,⊥,∥]

Laboratoire d'Utilisation du Rayonnement Electromagnétique, UMR No. 130, Université de Paris Sud, 91405 Orsay, France; Laboratoire de Physique des Milieux Désordonnés, Université Paris, XII–Val de Marne, 94010 Creteil, France; Laboratoire des Acides Minéraux et des Matériaux Inorganiques, URA CNRS No. 079, Université des Sciences et Techniques du Languedoc, 34095 Montpellier, France; Laboratoire de Chimie Inorganique, URA CNRS No. 420, Université de Paris Sud, 91405 Orsay, France; and Laboratoire des Sciences Moléculaires, Institut de Chimie de la Matière Condensée de Bordeaux, UPR CNRS No. 9048, avenue du Docteur Schweitzer, 33608 Pessac, France

Received February 23, 1995. Revised Manuscript Received July 6, 1995[⊗]

The goal of this paper is to obtain structural information on the compounds $[Fe(Htrz)_2(trz)](BF_4)$ (modifications **1a** and **1b**) and $[Fe(Htrz)_3](BF_4)_2 \cdot H_2O$ (**2**) with Htrz = 1,2,4-4*H*-triazole and trz = 1,2,4-triazolato. These compounds, in particular **1a**, exhibit cooperative spin transitions between low-spin (LS) and high-spin (HS) states around room temperature, with large thermal hysteresis and well-pronounced thermochromic effect. Both EXAFS spectroscopy at the iron K-edge and X-ray powder diffraction have been used. The EXAFS study has also been concerned with two model compounds, the crystal structures of which were known, namely, $[Fe_3(p\text{-MeOptrz})_8(H_2O)_4](BF_4)_6$ (**3**) and $[Fe_3(p\text{-MeOptrz})_6(H_2O)_6](tos)_6 \cdot 4H_2O$ (**4**), with *p*-MeOptrz = 4-*p*-methoxyphenyl-1,2,4-triazole and tos = tosylate. When the LS → HS transition occurs, as expected the length of the Fe–N bonds is increased by about 0.18 Å, and the FeN_6 core is more distorted. The spectra of all the compounds in the LS state show a very characteristic peak around 7 Å, which cannot be interpreted in the frame of the single scattering approach of the standard EXAFS formula. This peak has been assigned to a three-atom path involving aligned iron atoms. These EXAFS data perfectly agree with a linear chain structure for both **1** and **2**, with $Fe(Htrz)_6$ chromophores linked to each other through the 1,2 nitrogen positions of three triazole ligands. The stoichiometry of **1** requires a proton–hole disordered over each $Fe(Htrz)_2(trz)Fe$ bridging network. The X-ray data have provided two important pieces of information: first, the spin transition in both **1a** and **1b** most likely occurs without change of space group; second, the two modifications **1a** and **1b** do not crystallize in the same space group, the lattice symmetry of **1a** being lower. The relation between these structural data and the mechanism of the spin transition in these compounds is briefly discussed.

Introduction

The spin transition (ST) phenomenon was observed for the first time more than 50 years ago.[1] However, the interest raised by this phenomenon has seen a new impetus in the past two decades.[2–12] The ST phenomenon is probably the most spectacular example of bistability in molecular chemistry,[13] and one of our main concerns in this field of research deals with the possibility of using ST materials as active elements of devices for display or recording.[14–17] Along this line, we first defined five key requirements that a ST compound must fullfill for this purpose,[15] and then we explored some systems. Recently, we focused on the Fe(II)–Htrz system, with Htrz = 1,2,4-1*H*-triazole,[15,18] and characterized two compounds, namely, $[Fe(Htrz)_2(trz)]$-

† Laboratoire d'Utilisation du Rayonnement Electromagnétique.
‡ Laboratoire de Physique des Milieux Désordonnés.
§ Laboratoire des Acides Minéraux et des Materiaux Inorganiques.
⊥ Laboratoire de Chimie Inorganique.
∥ Laboratoire des Sciences Moléculaires.
⊗ Abstract published in *Advance ACS Abstracts,* September 1, 1995.

(1) Cambi, L.; Szegö, L. *Ber. Dtsch. Chem. Ges* **1931**, *64*, 259; **1933**, *66*, 656.
(2) Goodwin, H. A. *Coord. Chem. Rev.* **1976**, *18*, 293.
(3) Gütlich, P. *Struct. Bonding (Berlin)* **1981**, *44*, 83.
(4) König, E.; Ritter, G.; Kulshreshtha, S. K. *Chem. Rev.* **1985**, *85*, 219.
(5) Beattie, J. K. *Adv. Inorg. Chem.* **1988**, *32*, 1.
(6) Gütlich, P.; Hauser, A. *Coord. Chem. Rev.* **1990**, *97*, 1.
(7) König, E. *Prog. Inorg. Chem.* **1987**, *35*, 527.
(8) König, E. *Struct. Bonding (Berlin)* **1991**, *76*, 51.
(9) Gütlich, P.; Hauser, A.; Spiering, H. *Angew. Chem., Int. Ed. Engl.* **1994**, *33*, 2024.
(10) Adams, D. M.; Dei, A.; Rheingold, A. L.; Hendrickson, D. N. *J. Am. Chem. Soc.* **1993**, *115*, 8221.
(11) Roux, C.; Zarembowitch, J.; Gallois, B.; Granier, T.; Claude, R. *Inorg. Chem.* **1994**, *33*, 2273.
(12) Kahn, O. *Molecular Magnetism*; VCH: New York, 1993.
(13) Kahn, O.; Launay, J. P. *Chemtronics* **1988**, *3*, 140.
(14) Zarembowitch, J.; Kahn, O. *New J. Chem.* **1991**, *15*, 181.
(15) Kahn, O.; Kröber, J.; Jay, C. *Adv. Mater.* **1992**, *4*, 718.
(16) Jay, C.; Grolière, F.; Kahn, O.; Kröber, J. *Mol. Cryst. Liq. Cryst.* **1993**, *234*, 255.
(17) Kröber, J.; Codjovi, E.; Kahn, O.; Grolière, F.; Jay, C. *J. Am. Chem. Soc.* **1993**, *115*, 9810.

0897-4756/95/2807-1833$09.00/0

(BF_4) (**1**) and $[Fe(Htrz)_3](BF_4)_2 \cdot H_2O$ (**2**). Actually, two modifications of **1** were synthesized: **1a** prepared in a water/ethanol mixture, and **1b** prepared in pure methanol. **1a** exhibits a very abrupt transition between a low-spin (LS) and a high-spin (HS) state centered around 360 K with a thermal hysteresis that may reach 50 K, while **1b** exhibits a smoother transition with a smaller hysteresis. **2** was found to undergo a $\alpha \leftrightarrow \beta$ phase transition around 420 K. The α phase shows a rather abrupt spin transition centered around 335 K with a thermal hysteresis of about 20 K. The β phase is metastable at room temperature and shows a very abrupt spin transition around room temperature with a hysteresis width of a few kelvin. Three other groups, at least, are presently working on compounds of the same type.[19-22]

Compounds **1a** and **2** seem to exhibit ST regimes close to the ideal situation for their utilization in memory devices. **1a** possesses an extended bistability region with an hysteresis width of ca. 50 K; room temperature, however, does not fall within the hysteresis loop. **2** may offer an alternative way for solving this problem; in associating a crystallographic phase transition on one hand and a spin transition on the other hand, a system in which room temperature falls within the hysteresis loop may be obtained. Owing to their intrinsic interest, it was worth trying to obtain more information on the structure of the compounds and on the structural modifications accompanying the ST. That is the goal of this paper. The main structural questions we are faced with may be formulated as follows: (i) All the compounds, in particular **1a**, present a cooperative ST. We attributed the unusual cooperativity exhibited by these compounds to their polymeric nature, and for all the compounds we postulated a linear chain structure. Is it possible to confirm this hypothesis? (ii) Is the ST in these compounds accompanied by a crystallographic phase transition? (iii) Modifications **1a** and **1b** have strictly the same chemical analysis; there is no solvent molecule in the formula. Are the well-pronounced physical differences related to structural differences?

Despite many efforts, we did not succeed growing single crystals of **1** and **2** suitable for X-ray diffraction, and we decided to combine EXAFS spectra and X-ray powder patterns, in both the LS and HS states. The paper is organized as follows: First, the EXAFS spectra at the Fe K-edge of **1a**, **1b**, and **2** are compared to those of two model compounds, the structures of which are known, namely, $[Fe_3(p\text{-MeOptrz})_8(H_2O)_4](BF_4)_6$ (**3**) and $[Fe_3(p\text{-MeOptrz})_6(H_2O)_6](tos)_6 \cdot 4H_2O$ (**4**), with *p*-MeOptrz = 4-*p*-methoxyphenyl-1,2,4-triazole and tos = tosylate.[23] For both model compounds the structure consists of linear trinuclear cations with a +6 charge, noncoordinated anions, and solvent molecules. The molecular structure of the trinuclear cation in **3** is recalled in Figure 1. For **3** the three iron(II) ions are HS in the whole temperature range. For **4** the central iron(II) ion undergoes a gradual spin conversion centered at 245 K. Then, the X-ray diffractograms of **1a** and **1b** were investigated. The poor crystallinity of **2** did not allow us to obtain useful information concerning this compound. The last section is devoted to a discussion of the findings.

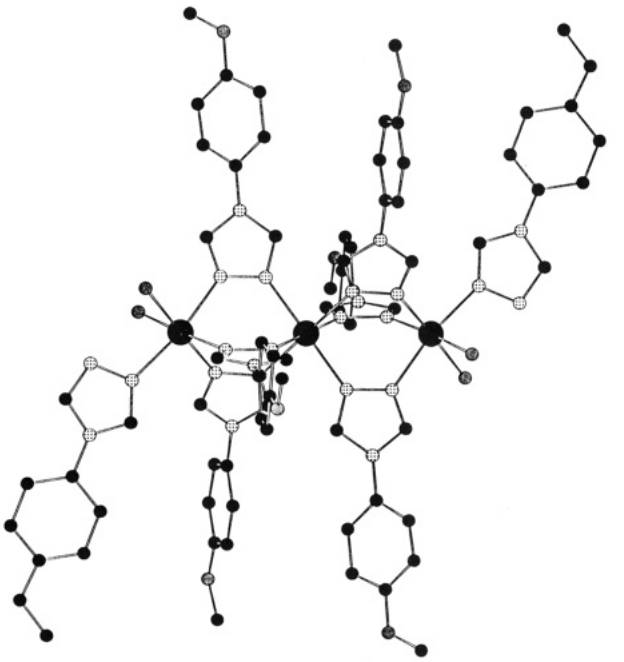

Figure 1. Molecular structure of the trinuclear cation $[Fe_3(p\text{-MeOptrz})_8(H_2O)_4]^{6+}$ in compounds **3** (from ref 23).

Experimental Section

Syntheses. The compounds $[Fe(Htrz)_2(trz)](BF_4)$ (**1a** and **1b**) and $[Fe(trz)_3](BF_4)_2 \cdot H_2O$ (**2**), the structures of which were unknown, were synthesized as previously described[18] and characterized through their magnetic properties. The model compounds utilized for the EXAFS study, namely, $[Fe_3(p\text{-MeOptrz})_8(H_2O)_4](BF_4)_6$ (**3**) and $[Fe_3(p\text{-MeOptrz})_6(H_2O)_6](tos)_6 \cdot 4H_2O$ (**4**) were also prepared as already described.[23]

EXAFS Data Collection and Analysis. The EXAFS spectra were recorded at LURE, the French synchrotron radiation facility, on the storage ring DCI (1.85 Gev, 300 mA). Two different X-ray absorption spectrometers were used in the transmission mode: EXAFS I, with a Si331 monochromator, and EXAFS III (Si311). Spectra reproductibility was checked by recording each sample on both EXAFS ports. The detectors were low pressure ($\approx$0.2 atm) air-filled ionisation chambers. Each spectrum is the sum of three recordings in the range 7080–8080 eV, including the iron K-edge ($\approx$7120 eV). The spectra were recorded at room temperature, 77 K with a liquid nitrogen cryostat, and 403 and 433 K (i.e., above the LS $\rightarrow$ HS transition) in a furnace designed for X-ray absorption spectroscopy. The samples were prepared as homogeneous compressed pellets with a mass calculated in order to obtain an absorption jump at the edge $\Delta\mu x \approx 1$ with a total absorption above the edge less than $\mu x \approx 1.5$.

The EXAFS data analysis was performed with the "EXAFS pour le MAC" programs[24] on a Macintosh personal computer. This standard EXAFS analysis[25-27] includes linear preedge

(18) Kröber, J.; Audière, J. P.; Claude, R.; Codjovi, E.; Kahn, O.; Haasnoot, J. G.; Grolière, F.; Jay, C.; Bousseksou, A.; Linarès, J.; Varret, F.; Gonthier-Vassal, A. *Chem. Mater.* **1994**, *6*, 1404.
(19) Haasnoot, J. G.; Vos, G.; Groeneveld, W. L. Z. *Naturforsch. B* **1977**, *32*, 421.
(20) Lavrenova, L. G.; Ikorskii, V. N.; Varnek, V. A.; Oglezneva, I. M.; Larionov, S. V. *Koord. Khim.* **1986**, *12*, 207.
(21) Lavrenova, L. G.; Ikorskii, V. N.; Varnek, V. A.; Oglezneva, I. M.; Larionov, S. V. *Koord. Khim.* **1990**, *16*, 654.
(22) Sugiyarto, K. H.; Goodwin, H. A. *Aust. J. Chem.* **1994**, *47*, 263.
(23) Thomann, M.; Kahn, O.; Guilhem, J.; Varret, F. *Inorg. Chem.* **1994**, *33*, 6029.
(24) Michalowicz, A. In *Logiciels pour la Chimie*; Société Française de Chimie: Paris, 1991; p 102.
(25) Teo, B. K. In *Inorganic Chemistry Concepts, EXAFS*; Springer-Verlag, Berlin, 1986; Vol. 9.
(26) Königsberger, D. C.; Prins, R. *X-Ray Absorption Principles, Applications, Techniques of EXAFS, SEXAFS and XANES*; John Wiley: New York, 1988.

background removal, polynomial and cubic spline atomic absorption calculation, Lengeler–Einsenberger EXAFS spectra normalization,[28] and reduction from the absorption data $\mu(E)$ to the EXAFS spectrum $\chi(k)$ with

$$k = \sqrt{(2m_e/h^2)(E - E_0)}$$

where E_0 is the energy threshold, taken at the absorption maximum. Radial distribution functions $F(R)$ were calculated by Fourier transforms of $k^3w(k)\,\chi(k)$ in the range 2–12.5 Å^{-1}; the experimental resolution is then $\pi/2\Delta k = 0.15$ Å. $w(k)$ is a Kaiser–Bessel apodization window with a smoothness coefficient $\tau = 2.5$. After Fourier filtering, the first single-shell FeN_6 was fitted to the standard EXAFS formula, without multiple scattering:

$$k\chi(k) = -S_0{}^2(N/R^2)|f(\pi,k)|e^{-2\sigma^2k^2}e^{-2R/\lambda(k)} \times \sin[2kR + 2\partial_1(k) + \psi(k)]$$

were $S_0{}^2$ is the inelastic reduction factor ($S_0{}^2 = 1$ in our fits), N is the number of nitrogen atoms at the distance R from the iron center, $\lambda(k) = k/\Gamma$ is the mean-free path of the photoelectron (Γ is fitted to the value 1.245 Å^{-2} in order to obtain exactly $N = 6$ for **1a** at 77 K, and this value is kept constant for all the other fits), σ is the Debye–Waller coefficient, characteristic of the width of the Fe–N distance distribution, $\partial_1(k)$ is the central atom phase shift, and $|f(\pi,k)|$ and $\psi(k)$ are the amplitude and phase of the nitrogen backscattering factor, respectively. The spherical-waves theoretical amplitudes and phase shifts calculated by McKale[29] and amplitudes and phase shifts extracted from the computer program FEFF[30–34] were used. As expected for single backscattering fits, the differences between both sets of results are always within the error bars. Since theoretical phase shifts were utilized, it was necessarry to fit the energy threshold E_0 by adding an extra fitting parameter ΔE_0. The single-shell model is only valid when the width of the Fe–N distance distribution is smaller than the experimental resolution. For one sample (**4** at 77 K) the first peak filtered spectrum exhibits a clear beating characteristic of a resolved two-shell system and therefore could not be fitted with only one Fe–N distance. This filtered spectrum was then fitted with two independent Fe–N distances. The goodness of fit is given by

$$\varrho(\%) = \Sigma[k\chi_{exp}(k) - k\chi_{th}(k)]^2/\Sigma[k\chi_{exp}(k)]^2$$

As recommended by the International Workshop on Standards and Criteria in XAS,[27] we performed an analysis of the error bars of the fitted parameters. The average experimental signal/noise ratio was found to be better than 20, and the fitted parameters standard error bars were significantly less than the commonly accepted systematic errors: 0.01 Å for the distance and 20% for the number of nearest neighbors. In this work, the later error bars were finally adopted.

The modeling of the outer shells was not possible in the frame of the single scattering model, and the multiple scattering/spherical-waves EXAFS ab initio modeling FEFF program was used.[30–34] These calculations were performed on the DEC7620 Alpha Computer of the central Computing Department of LURE.

X-ray Patterns. These were recorded with a laboratory-made apparatus consisting of a θ–2θ goniometer and a temperature-controlled chamber. A Cu Kα anticathode was used. The system comprises an accumulation option, which allows the study of poorly crystallized materials. Compounds **1a** and **1b** were investigated in detail in the form of compacted powder samples. An argon flow was used to prevent the oxidation. The diffractograms were obtained by an accumulation of 20 runs. They were recorded every 10 K between room temperature and 420 K for **1a** and **1b** and between room temperature and 450 K for **2**, in both the warming and cooling modes. Compound **2** both in the α and β forms is poorly crystallized, and the X-ray study did not bring useful information. The diffractograms of **2**, however, are given in the supporting information.

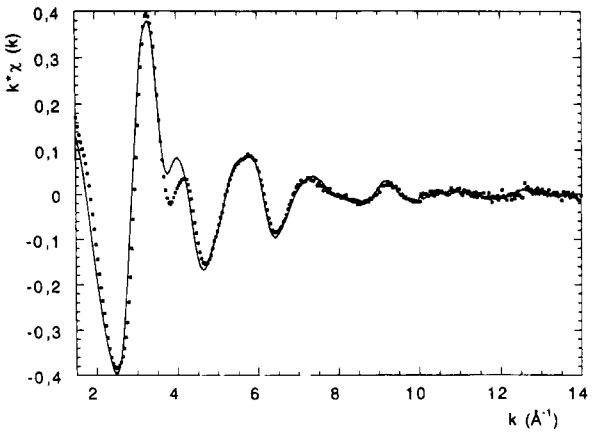

Figure 2. Comparison of the EXAFS data for **1a** at 403 K (■) and **3** at room temperature (—).

EXAFS Study

Qualitative Analysis. The complete set of EXAFS spectra, namely, $k\chi(k)$ and Fourier transforms $|F(R)|$ and $Im(F(R))$ of the model compounds **3** and **4** as well as of the compounds of unknown structures **1a**, **1b**, and **2** at various temperatures are provided as supporting information.

These spectra can be classified into two distinct subsets of similar data: one subset deals with compounds **1a**, **1b**, and **2** in the LS state; the other one deals with all the compounds **1**–**4** in the HS state. The spectrum of **4** at 77 K does not belong to any of these subsets. Indeed, at that temperature, the two terminal iron(II) ions are HS and the central iron(II) ion is LS.[23] The similarity of the spectra when the iron(II) ions are in the HS state allows us to assume that the local structures of the HS iron(II) ions are very close to each other. This situation is illustrated in Figure 2, where the EXAFS spectra of **1a** at 403 K and **3** at room temperature are compared. Furthermore, the spectra of the compounds for which all the iron(II) ions are LS are also very close to each other, suggesting again that the local structures in the LS state are almost identical.

The EXAFS spectra of **1a** in both the LS and HS states are represented in Figure 3a, whereas the Fourier transforms of these spectra are drawn in Figure 3b,c, respectively. When the LS → HS transition occurs, the frequency of the EXAFS signal increases, reflecting the lengthening of the Fe–N bonds. The damping of the EXAFS signal also increases; the iron first coordination sphere is more distorted in the HS than in the LS state. Differences between LS and HS local structures can be also discussed by comparing the Fourier transforms modulus ($|F(R)|$) of the spectra, normalized to their main maxima (see Figure 3b,c). Comparing Fourier trans-

(27) Lytle, F. W., Sayers, D. E., Stern, E. A., Co-Chairman; *Report of the International Workshop on Standards and Criteria in X-Ray Absorption Spectroscopy*; *Physica* **1989**, *B158*, 701.
(28) Lengeler, B.; Eisenberger, P. *Phys. Rev.* **1980**, *B21*, 4507.
(29) McKale, A. G. *J. Am. Chem. Soc.* **1988**, *110*, 3763.
(30) Rehr, J. J.; Zabinsky, S. I.; Albers, R. C. *Phys. Rev. Lett.* **1992**, *69*, 3397.
(31) Rehr, J. J. *Jpn J. Appl. Phys.* **1993**, *32*, 8.
(32) Rehr, J. J.; Mustre de Léon, J.; Zabinsky, S. I.; Albers, R. C. *J. Am. Chem. Soc.* **1991**, *113*, 5135.
(33) Mustre de Léon, J.; Rehr, J. J.; Zabinsky, S. I.; Albers, R. C. *Phys. Rev.* **1991**, *B44*, 4146.
(34) Rehr, J. J.; Albers, R. C. *Phys. Rev.* **1990**, *B41*, 8139.

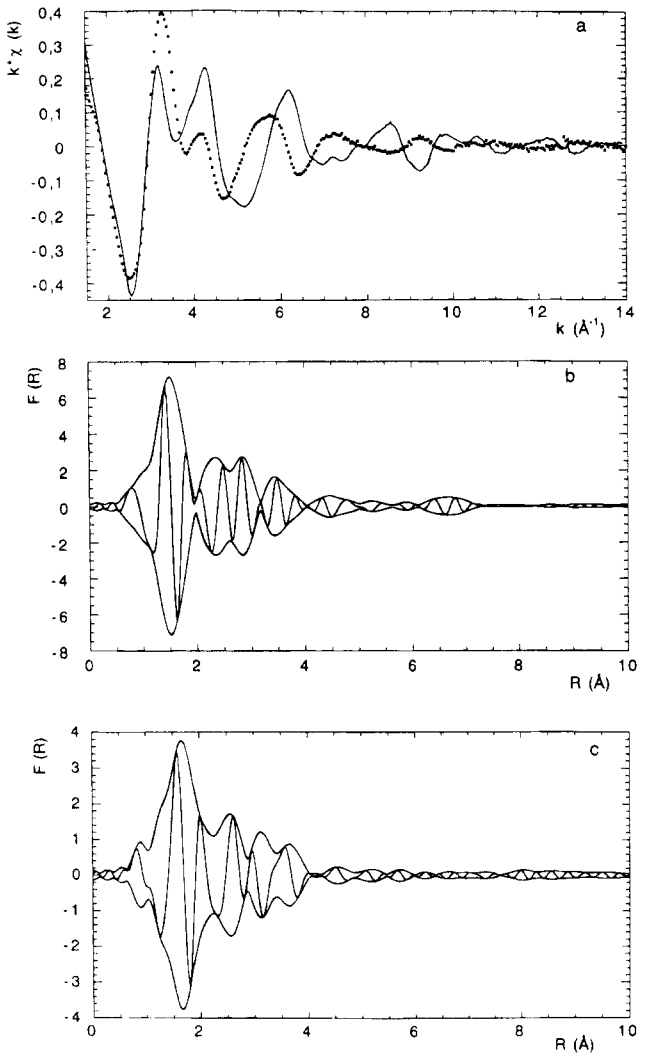

Figure 3. (a) Comparison of the EXAFS spectra for **1a** at room temperature in the LS state (■) and 403 K in the HS state (—); (b) Fourier transform of the LS spectra; (c) Fourier transform of the HS spectrum.

form spectra without normalization is difficult since the distortion of the coordination sphere leads to a decrease of $F(R)$ by a factor 2. Both spectra comprise four main peaks. The more distorted character of the iron(II) coordination sphere in the HS state is confirmed by a decrease of the amplitude of the Fourier transform and an increase of the width of the first peak. Thus, this peak strongly overlaps with the second one. Despite these differences the two EXAFS spectra are characteristic of the same local structure. The modulus of the Fourier transform of the spectra of **1a** in LS and HS states are superimposed in Figure 4. To the eye, it clearly appears that the four main peaks in the radial distribution functions are almost the same with a significant lengthening in the Fe–N bonds. The magnitude of this lengthening will be determined in the quantitative analysis section. This qualitative comparison between LS and HS radial distribution functions proves that the mode of coordination of the triazole ligand is not drastically changed between HS and LS states. The only modification in the peaks lying between 1.5 and 5 Å is the expected change in the Fe–ligand bond lengths. Another difference between LS and HS spectra is the presence of a small long-distance peak near 7 Å in the former, which vanishes in the

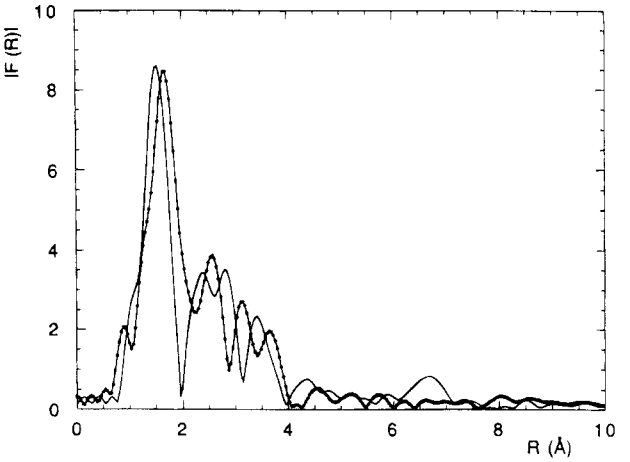

Figure 4. Superposition of the normalized modulus of the Fourier transforms in **1a** in LS and HS states.

latter. This peak is visible in all the LS spectra; its origin will be discussed below. However, since the presence of this peak will provide some crucial information on the structures of compounds **1** and **2**, it appeared to us that it was necessary to prove unambiguously that this peak is not due to an artifact. Actually, four kinds of possible artifacts were considered, namely,

(i) Background Removal Drawback. It is well-known that such numerical drawbacks can add some spurious low-frequency peaks (R < 1 Å).[25,26] Actually, a 7 Å signal in the background could be easily detected. Indeed, the EXAFS program we use allows us to analyze the background by Fourier transform and to remove it from the absorption curve. It was carefully checked that in the present case there is no spurious signal around 7 Å in the background of the spectra. Furthermore, a Fourier analysis of the EXAFS spectra definitely proved that the 7 Å peak discussed here actually belongs to the experimental signal and not to the mathematical background. The EXAFS signal of compound **1** at 77 K, extracted with a linear background, is plotted in Figure 5a. Such a linear background is not adequate for a complete EXAFS analysis, but useful to prove that the high-frequency oscillations are present in the 7–9 Å range of the experimental curve. Two filtered EXAFS spectra are represented in Figure 5b, namely, the R < 6.3 Å filter and the R < 7.3 Å filter, along with the difference between these two spectra. The former spectrum represents the EXAFS spectrum without the contribution of the 7 Å peak, and the latter spectrum includes this peak. This analysis clearly establishes the relation between the 7 Å peak and the experimental oscillations in the 7–9 Å range. It can also be noticed that this long-distance peak is not so weak as compared to the lower distance contributions.

(ii) Noisy Spectra. It is clear from the Fourier transform spectra of LS species (Figure 3b) that the peak at 7 Å is largely above the noise level. A signal due to the noise should not appear at a constant frequency. Furthermore, the HS spectra are more noisy than the LS ones, although no feature around 7 Å can be seen on the related spectra.

(iii) X-ray or Monochromator Artifacts. Accidental fluctuations of the X-ray intensity can lead to oscillations that are not structurally relevant. We carefully checked that such fluctuations are observed, neither in the incoming beam I_0 nor in the transmitted beam I.

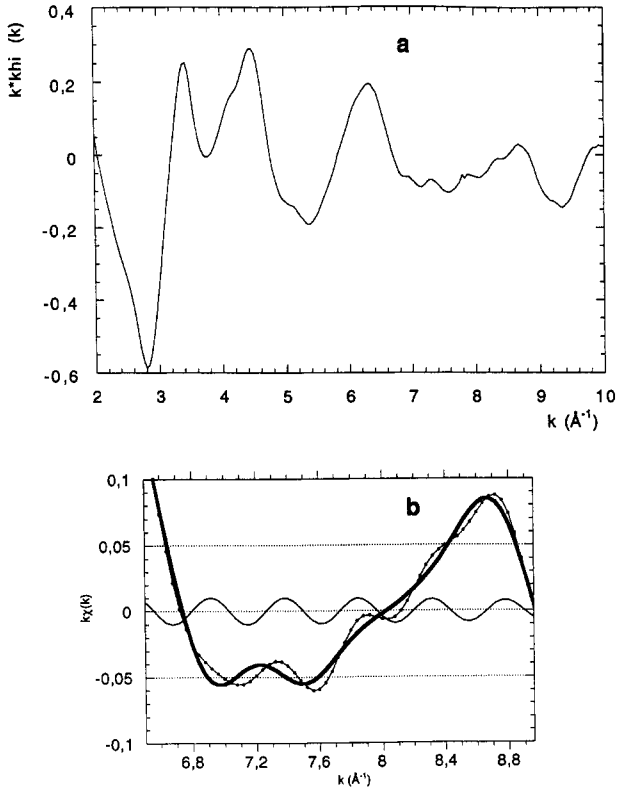

Figure 5. Analysis of the high-frequency contribution (around 7 Å) to the EXAFS spectrum of compound **1** at 77 K. (a) EXAFS spectrum calculated with a linear background. (b) filtered spectrum in the 7–9 Å range for R < 6.3 Å filter (thick line), R < 7.3 Å filter (dotted line), difference spectrum (thin line).

Moreover, our spectra were recorded three times with a 1-month interval, and with two different monochromators. The reproductibility of the 7 Å peak, present only in the LS spectra, definitely eliminates this kind of artifact.

(iv) Sample Inhomogeneity and Cracks. Each set of data was recorded with newly prepared samples. HS and LS sample quality and homogeneity were carefully checked and found to be equivalent. Cryostat fluctuations can also be ruled out since the crucial structure is also seen on LS spectra at room temperature.

To sum up the preceding discussion, we can say that the 7 Å signal is not due to an experimental or mathematical artifact but arises from the structure of the compounds. Such a long-distance contribution is not exceptional in EXAFS. However, its intensity is usually weak with respect to the noise level. An isolated peak at 7 Å can be observed only when the following requirements are fulfilled: (i) The number of identical sites sitting at the corresponding distance from the absorbing center should not be too small. (ii) The contributing atoms should be strongly bonded, which results in a weak Debye–Waller factor. These long-distance peaks are particularly sensitive to structural or thermal disorder.[35] At room temperature, a 7 Å contribution cannot be due to intermolecular interactions. Metal ions in a polymeric structure are good candidates to provide intramolecular signals and long-distance peaks. (iii) If the distance is exactly twice the Fe–Fe separation between adjacent ions, then the signal must be concerned with the multiple scattering effect. It is well established that the main effect of multiple scattering is to enhance dramatically the amplitude of the signal, in particular when the central atom and its two neighbors are aligned.[25,26] A quantitative analysis of this phenomenon was impossible until multiple scattering-spherical wave EXAFS codes became available. Putting all together these arguments, it is possible to suggest that the 7 Å peak observed in the LS state arises from a Fe–Fe–Fe alignment.

(35) Michalowicz, A.; Verdaguer, M.; Mathey, Y.; Clement, R. In *Topics in Current Chemistry*; Springer-Verlag: Berlin, 1988; Vol. 145.

Table 1. Fitting of the First Coordination Sphere of the EXAFS Data for Compounds 1–4

sample	N	$10^2\,\sigma$(Å)	R (Å)	ΔE_0 (eV)	ϱ (%)
1a, 403 K, HS	6.0 (1.2)	9.7	2.16 (1)	−1.4	1.8
1a, 298 K, LS	6.0 (1.2)	6.8	1.99 (1)	−3.8	1.8
1a, 77 K, LS	6.0 (1.2)	5.7	1.98 (1)	−3.9	2.5
1b, 403 K, HS	6.0 (1.2)	9.9	2.18 (1)	−0.5	2.3
1b, 298 K, LS	5.6 (1.1)	6.4	1.99 (1)	−2.4	4.9
1b, 77 K, LS	6.2 (1.2)	5.5	1.99 (1)	−3.0	2.9
2, 433 K, HS	6.5 (1.3)	0.1	2.17 (1)	−1.7	1.8
2, 403 K, HS	6.2 (1.2)	9.3	2.18 (1)	0.1	1.7
2, 298 K, LS	5.6 (1.1)	6.4	1.99 (1)	−2.3	2.1
2, 77 K, LS	5.5 (1.1)	6.3	1.99 (1)	−1.9	2.5
3, 298 K, HS	7.0 (1.4)	10	2.18 (1)	−0.9	1.3
3, 77 K, HS	7.0 (1.4)	9.4	2.18 (1)	0.1	1.3
4, 403 K, HS	7.2 (1.4)	10	2.15 (1)	−3.9	1.2
4, 298 K, HS	7.0 (1.4)	12	2.09 (1)	−5.3	1.7
4, 77 K, HS	2.8 (6)	7.0	2.02 (2)	−1.4	7.0
	3.2 (6)	7.0	2.18 (2)	−1.4	

Quantitative Analysis. We have seen that all the LS spectra on the one hand, and all the HS spectra on the other hand are very close to each other. Table 1 gives the fitting results for the first coordination sphere of compounds **1–4** at 77 K, room temperature, and above the LS → HS transition. For compound **2** the results obtained at 433 K, i.e., above the $\alpha \rightarrow \beta$ phase transition, are also presented. The complete results are availale as supporting information. The data of this Table 1 confirm the qualitative discussion: the LS → HS transition results in a lengthening of about 0.18 Å in the Fe–N bonds, accompanied with a significant increase of the Debye–Waller coefficient which is almost doubled. The Fe–N bond length distributions for compounds **1** and **2** are found to be larger in the HS than in the LS state, reflecting the Jahn–Teller instability of the orbitally degenerate $^5T_{1g}$ state.

A complete quantitative discussion of the local structure around the Fe(II) ion including atoms in a sphere of 8 Å cannot be correctly performed in the frame of the single-scattering approach of the standard EXAFS formula. The reason of this difficulty is obvious if one carefully looks at the local environment of the central atom (see Figure 6). Beyond the single backscattering paths (nleg = 2, nleg being the number of scattering segments in the FEFF program) a lot of three-atom paths (nleg = 3 and 4) with scattering angles close to 180° can be seen. Some pathways with nleg > 4 are also significant and cannot be neglected. In Figure 7a the imaginary part of the radial distribution functions for the model compound **3** at 77 K is compared to the FEFF theoretical model including almost 150 scattering paths, calculated by FEFF on the complete set of atomic coordinates given in ref 23. In the HS model the theoretical EXAFS spectrum corresponding to the central and terminal iron(II) ions has been calculated. The final spectrum is calculated as the weighted $\chi = (\chi_{central}$

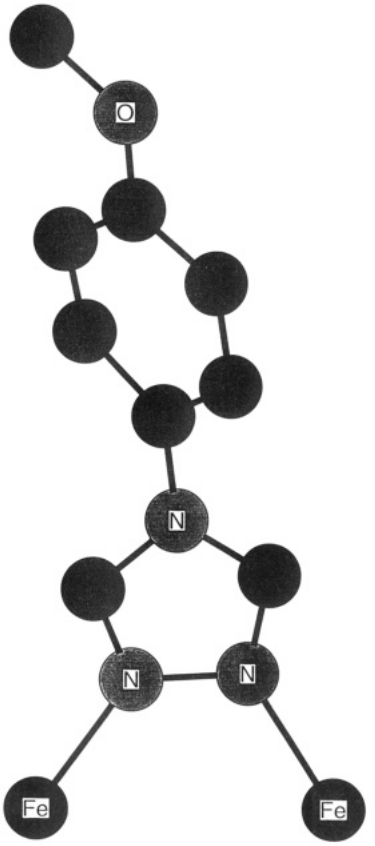

Figure 6. Local environment of the iron atom emphasizing the three-atom paths with scattering angles close to 180°.

$+ 2\chi_{terminal})/3$. The large number of pathways determined by FEFF is due to the fact that the symmetry of compound **3** is low and that the degeneracy is weak. For the LS FEFF model a symmetrical structure with perfect octahedral surroundings around the iron(II) ions is used. In that case the number of pathways calculated by FEFF is 80. The two spectra compare quite well, in both phase and amplitude. The quality of the FEFF model compared to the experimental spectrum is also illustrated in Figure 7b showing the two spectra in the k space. On the other hand, if a FEFF model with only single-scattering paths is used, it is clear that the experimental and calculated spectra are not in phase anymore beyond the first coordination sphere (see Figure 7c). One important point of this FEFF study is that above 3 Å the contributions of the scattering paths are largely overlapping and cannot be separated between the observed peaks. For example, it is impossible to attribute one particular Fourier transform peak to the Fe−Fe contribution at 3.87 Å.

With the use of FEFF it is now possible to come back to the peak around 7 Å in the spectra of **1a**, **1b**, and **2** in the LS state. Figure 8 shows a FEFF model of such a LS structure where the Fe−Fe distance was fixed to 3.65 Å (Fe−Fe−Fe = 7.30 Å). With this Fe−Fe separation FEFF theoretical multiple scattering and experimental peaks match quite well, in both position and phase. The multiple scattering Fe−Fe−Fe signal is clearly identified (arrow). The problem we are faced with now is to understand why this signal is seen neither in the spectra of the trinuclear model compounds **3** and **4** nor in the spectra of compounds **1** and **2** in the HS state. In the case of the trinuclear species this absence of Fe−Fe−Fe signal may be interpreted

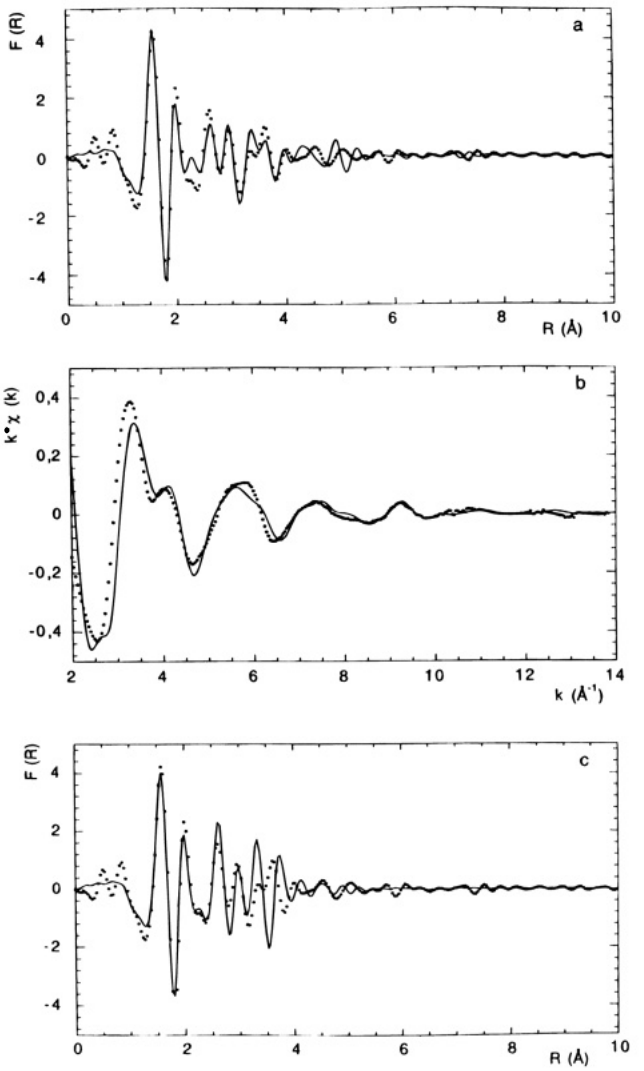

Figure 7. Comparison between the experimental spectrum for **3** at 77 K and the calculated spectrum using the FEFF method, including scattering paths up to 8 Å: (a) imaginary parts of the Fourier transforms; (b) k-space spectra; (c) same FEFF calculation but with only single backscattering paths. (···) experimental curve; (—) FEFF model.

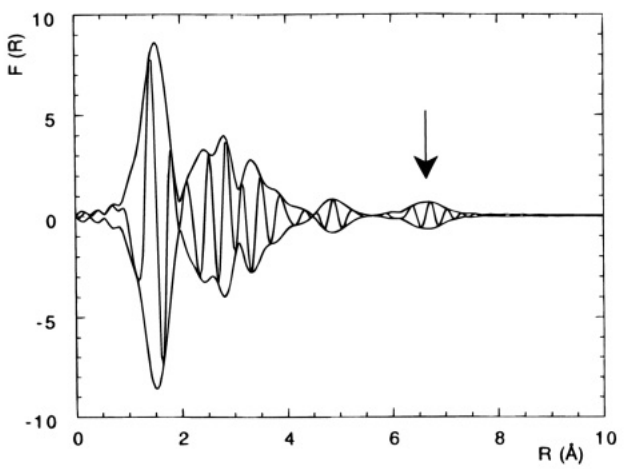

Figure 8. Fourier transform of a complete FEFF calculation for compound **3** including Fe−Fe−Fe multiple scattering paths.

as follows: The two external iron atoms are concerned only with one Fe−Fe−Fe multiple-scattering signal, and the central iron atom does not see any metal neighbor at 2 × 3.87 Å. Therefore, the multiple-scattering Fe−

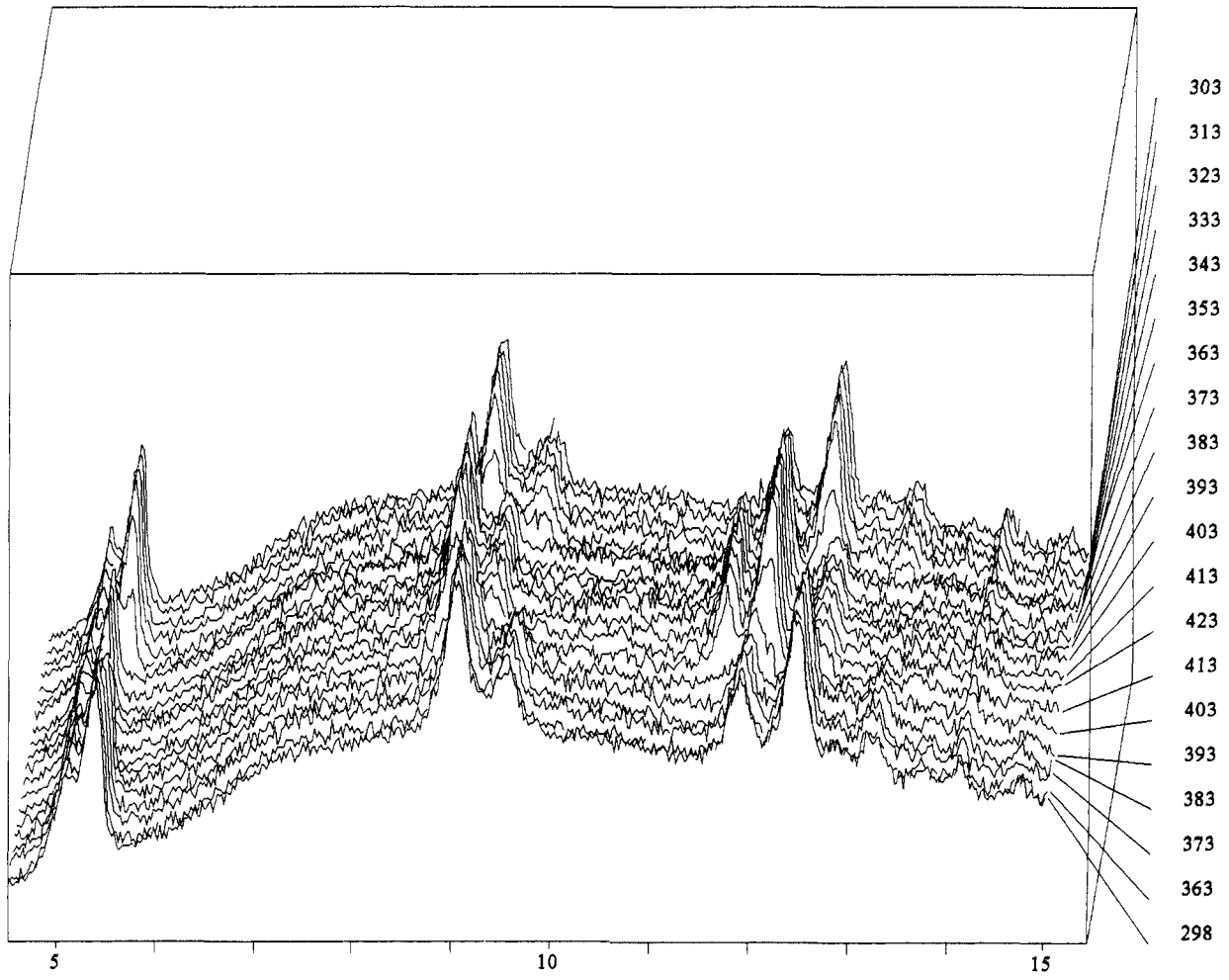

Figure 9. Diffractograms of **1a** in the 4.5° < θ < 15° range recorded every 10 K between 363 and 423 K in the warming mode, and between 423 and 303 K in the cooling mode.

Fe–Fe signal is 3 times smaller than for an infinite linear chain and probably lower than the background level. It can be seen that the Fe–Fe–Fe multiple scattering signal around 7 Å as obtained in the FEFF model is significantly weaker for a HS trinuclear compound (see Figure 7a) than for a LS linear chain compound (see Figure 8). The absence of multiple scattering signal around 7 Å in the HS state of compounds **1** and **2** is more difficult to understand. We can invoke three reasons for this lack of signal: (i) The linear chain is destroyed during the LS → HS transition. If such a possibility cannot be ruled out from the EXAFS data, it is obviously irrelevant. (ii) The chains are still present but are not linear anymore, which could be a consequence of the Jahn–Teller distortion in the HS state. (iii) Since the HS spectra of compounds **1** and **2** are recorded at high temperature, the Fe–Fe–Fe network is subject to important thermal vibrations leading to a Debye–Waller factor that cancels the corresponding signal. This third hypothesis seems to us to be the most probable. The second hypothesis, however, cannot be completely ruled out.

From the qualitative and quantitative analyses of the EXAFS data it is now possible to give a rather accurate description of the structure of compounds **1** and **2**. The local structure of the Fe(II) ion in **1** and **2** is very close to that of the central Fe(II) ion in the trinuclear compound **4**, with almost the same Fe–N bond lengths. The ST is accompanied by an expected increase of the average Fe–N distance along with a significant distortion of the FeN_6 octahedron; the main features of the local structure, however, are retained. Finally, and this is the most important result, the EXAFS spectra of compounds **1** and **2** in the LS state definitely prove that compounds **1** and **2** have a linear chain structure, at least in this LS state.

X-ray Study

Compound 1a. Figure 9 shows the diffractograms of **1a** at various temperatures, and Table 2 lists the θ and d values of the diffraction peaks in both the LS and HS states. The spin transition, detected through the abrupt change of position of the peaks, was observed around $T_c\uparrow$ = 405 K in the warming mode, and $T_c\downarrow$ = 360 K in the cooling mode. The thermal hysteresis width is therefore of the order of 45 K, which agrees with the magnetic calorimetric, optical, and Mössbauer measurements.[18,22] Several thermal cycles were successively carried out, and the transition temperatures remained unchanged, in both the warming and cooling modes. The diffractograms recorded at room temperature before and after the thermal treatments are strictly identical, even after several thermal cycles, which confirms the nonfatiguability of the spin transition materials.[15]

Let us now compare the diffractograms in the LS and HS states. These diffractograms are actually quite

Table 2. θ (deg) and d (Å) Values and Relative Intensities (vs = Very Strong, s = Strong, m = Medium) of the Diffraction Peaks for 1a and 1b

θ (deg)	d (Å)	intensity
	1a at 298 K	
5.20	8.499	m
5.48	8.007	vs
9.16	4.838	s
9.70	4.571	m
12.02	3.699	s
12.58	3.536	vs
13.38	3.329	m
	1a at 413 K	
5.19	8.515	m
5.36	8.246	vs
9.00	4.924	s
9.62	4.609	m
11.74	3.818	s
12.16	3.657	vs
12.60	3.531	m
	1b at 303 K	
5.38	8.215	s
9.28	4.776	s
12.38	3.593	vs
13.32	3.343	s
	1b at 413 K	
5.34	8.276	s
9.25	4.792	s
12.06	3.686	vs
12.72	3.498	s

similar as far as both the number of peaks and their relative intensities are concerned (see Figure 9 and Table 2). The LS → HS transition, however, is accompanied by an important dilatation of the crystal lattice. These findings suggest that the spin transition takes place without crystallographic phase transition. However, some diffraction peaks with a very weak intensity might be hidden by the background; some of these peaks might appear and disappear with the occurrence of the spin transition. It follows that it is not possible to assert with an absolute certainty that the space group is retained.

Compound 1b: Comparison with 1a. 1b behaves much in the same way as **1a** (see Figure 10 and Table 2). The transition temperatures, however, are lower, and the thermal hysteresis width is weaker, in agreement with the previous measurements.[18]

The important point concerns the structural differences, if any, between **1a** and **1b**. Actually, both in the LS and HS states the diffractograms of **1a** and **1b** are not identical, as shown in Figure 11. More precisely, there are more diffraction peaks for **1a**. These additional peaks may be described as resulting from a doubling of the peaks of **1b**. Most probably, the two crystal lattices are close to each other, with a lower symmetry for **1a**.

Discussion

At the end of the Introduction, we stated three questions concerning the structure of the ST materials in the Fe(II)–Htrz system. What we would like to do here is to discuss each of the answers brought about by this work.

The first and main question dealt with the basic structure of compounds **1** and **2**. It has been suggested that **2** has a linear chain structure with octahedral Fe(Htrz)$_6$ chromophores linked to each other through the 1,2 nitrogen positions of three triazole ligands as schematized in Figure 12.[18] The local structure of each iron(II) ion in **2** would be very close to that of the central metal ion of the trinuclear species **3** and **4**. The EXAFS data entirely confirm this hypothesis. Moreover, they indicate that the Fe–N bonds are about 0.18 Å longer in the HS than in the LS state and that the LS → HS transition is accompanied by a distortion of the FeN_6 octahedron. These findings concerning the Fe–N bond lengths and the symmetry of the FeN_6 chromophore are obviously not surprising. The same modifications have been found through single-crystal X-ray diffraction for quite a few mononuclear iron(II) ST compounds[7,36] and for the central iron(II) ion of a trinuclear species.[37]

The same kind of linear chain structure has also been postulated for **1**, which requires a proton hole disordered over each Fe(Htrz)$_2$(trz)Fe bridging network. Again, the EXAFS data are in line with this hypothesis. Actually, the EXAFS spectra for **1a**, **1b**, and **2** in the same spin state are almost identical. Our results allow to rule out the hypothesis that the deprotonated triazolato group would be triply bridging through its three nitrogen atoms as observed in some Ru(II)–trz organometallic compounds[38] and Zn(trz)Cl.[39]

The knowledge of the basic structure of these materials raises a new question: what is the intimate relation between the strong cooperativity and the polymeric nature? In other terms, what is the real mechanism of the cooperativity in such compounds? Is this mechanism of the same nature as that of the cooperativity in more classical ST compounds where mononuclear entities are weakly connected through hydrogen bonds? We hope to be able to bring interesting insights on this problem in a subsequent paper.

The second question dealt with the structural transformations accompanying the ST. Our X-ray data suggest that the ST in **1a** and **1b** takes place without change of space group. For each modification the diffractograms in the LS and HS states are very close to each other; the number and the relative intensities of the peaks are unchanged. Just a dilatation of the lattice is observed when passing from the LS to the HS state. The fact that the space group is retained has to be considered as a strong probability and not as an absolute certainty. Some weakly intense peaks revealing a phase transition could be hidden by the background. It is worth reminding that some years ago it was believed that the occurrence of a thermal hysteresis necessarily required a crystallographic phase transition and vice versa.[40–42] Actually, **1a** exhibits one of the most abrupt ST observed so far, with a beatifully square-shaped thermal hysteresis loop, and probably retains the same space group in both spin states. The enthalpy variation accompanying the ST in **1a** is exceptionally large; it has been found to be equal to

(36) Gallois, B.; Real, J. A.; Hauw, C.; Zarembowitch, J. *Inorg. Chem.* **1990**, *29*, 1152.
(37) Vos, G.; de Graaff, R. A. G.; Haanoot, J. G.; van der Kraan, A. M.; de Vaal, P.; Reedijk, J. *Inorg. Chem.* **1984**, *23*, 2905.
(38) Oro, L. A.; Pinillos, M. T.; Tejel, C.; Foces-Foces, C.; Cano, F. H. *J. Chem. Soc., Dalton Trans.* **1986**, 1087; **1986**, 2193.
(39) Kröber, J.; Bkouche-Waksman, I.; Pascard, C.; Thomann, M.; Kahn, O. *Inorg. Chim. Acta* **1995**, *230*, 159.
(40) Ganguli, P.; Gütlich, P.; Müller, W.; Irler, W. *J. Chem. Soc., Dalton Trans.* **1981**, 441.
(41) Müller, E. W.; Spiering, H.; Gütlich, P. *Chem. Phys. Lett.* **1982**, *93*, 567.
(42) Wiehl, L.; Kiel, G.; Köhler, C. P.; Spiering, H.; Gütlich, P. *Inorg. Chem.* **1986**, *25*, 1565.

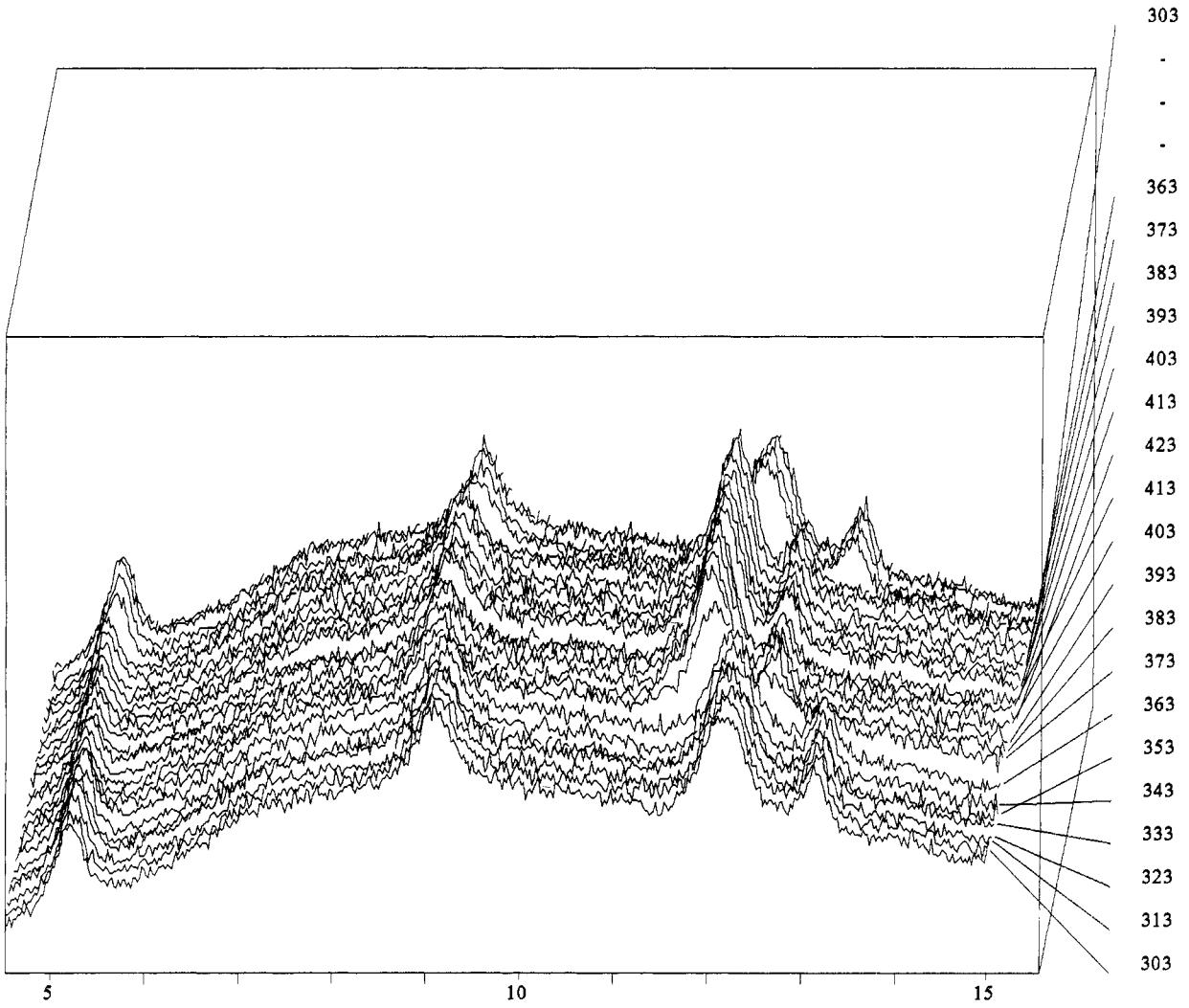

Figure 10. Diffractograms of **1b** in the 4.5° < θ < 15° range recorded every 10 K between 303 and 423 K in both the warming and cooling modes.

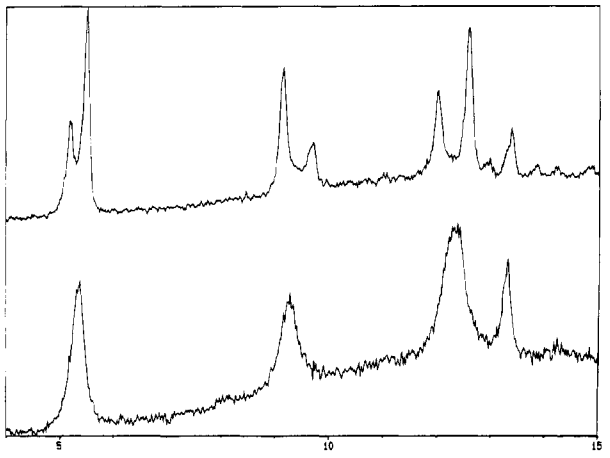

Figure 11. Comparison of the diffractograms of **1a** (top) and **1b** (bottom) in the 4.5° < θ < 15° range at room temperature.

about 27 kJ mol^{-1}. This magnitude of the enthalpy variation does not seem to be due to a change of space group. Perhaps, the modification of the iron(II) coordination sphere requires more energy in a polymeric than in a purely molecular lattice.

The third and last question dealt with the structural differences between **1a** and **1b**. Let us recall that these two modifications are prepared in different solvents but have strictly the same chemical formula; there is no solvent molecule in the lattice. When writing our previous paper on these compounds,[18] we were quite astonished by the differences of physical properties between the two modifications. The situation now is clear. **1a** and **1b** do not crystallize in the same space group. The lattice symmetry of **1a** is lower than that of **1b**. The last point remaining to understand is why a lower lattice symmetry results in a more abrupt transition and a larger hysteresis loop.

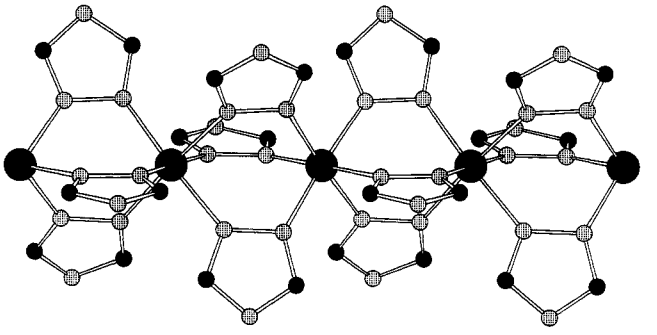

Figure 12. Structure of compounds **1** and **2**, as deduced from this work (see text).

Conclusion

At the end of this work we would like to emphasize in a few words that these compounds [Fe(Htrz)$_2$(trz)]-

(BF_4) and $[Fe(Htrz)_3](BF_4)_2 \cdot H_2O$ are fascinating and yet have not revealed all their secrets. The abruptness and the very large thermal hysteresis for **1a** most likely result from the polymer nature of the compound, which has been confirmed for the first time in this work. The presence of chemical bridges between the iron(II) ions induces an exceptionally strong cooperativity. It has been shown in a recent paper that the cooperativity in such one-dimensional ST compounds essentially arises from the intrachain and not the interchain interactions. Increasing the length and the bulkiness of the R substituent on the 4-position of $[Fe(Rtrz)_3](tos)_2$ compounds does not modify significantly the hysteresis width.[43] It remains to understand why the cooperativity is even more pronounced in compound **1** in which one of the triazole ligands is deprotonated. One of our main goals in the near future is to analyze the mechanism of the cooperativity in these polymeric ST molecules.

(43) Armand, F.; Badoux, C.; Ruaudel-Texier, A.; Kahn, O. *Langmuir*, in press.

Supporting Information Available: θ and d values, relative intensities, and diffractograms for **2** (2 pages). Ordering information is given on any current masthead page.

Acknowledgment. We are very grateful to the staffs of the linear accelerator and storage ring at LURE. We would also like to express our gratitude to Drs. P. Parent, A. Traverse, and A. Sadoc for the use of the EXAFS 1 and 3 spectrometers, to Dr. F. Villain for the sample preparation and the use of the cryogenic devices and furnace, and to Mrs. D. Michalowicz from the Computing Department of LURE for her help in the use of the FEFF program.

CM950091C